An ALMA survey of submillimetre galaxies in the Extended Chandra Deep Field South: high-resolution 870 μm source counts

A. Karim,[1]⋆ A. M. Swinbank,[1] J. A. Hodge,[2] I. R. Smail,[1] F. Walter,[2] A. D. Biggs,[3]
J. M. Simpson,[1] A. L. R. Danielson,[1] D. M. Alexander,[1] F. Bertoldi,[4] C. de Breuck,[3]
S. C. Chapman,[5] K. E. K. Coppin,[6] H. Dannerbauer,[7] A. C. Edge,[1] T. R. Greve,[8]
R. J. Ivison,[9,10] K. K. Knudsen,[11] K. M. Menten,[12] E. Schinnerer,[2] J. L. Wardlow,[13]
A. Weiß[12] and P. van der Werf[14]

[1]*Institute for Computational Cosmology, Durham University, South Road, Durham DH1 3LE, UK*
[2]*Max-Planck-Institut für Astronomie, Königstuhl 17, D-69117 Heidelberg, Germany*
[3]*European Southern Observatory, Karl-Schwarzschild Strasse 2, D-85748 Garching, Germany*
[4]*Argelander-Institute of Astronomy, Bonn University, Auf dem Huegel 71, D-53121 Bonn, Germany*
[5]*Institute of Astronomy, University of Cambridge, Madingley Road, Cambridge CB3 0HA, UK*
[6]*Department of Physics, McGill University, 3600 Rue University, Montreal, QC H3A 2T8, Canada*
[7]*Institut für Astrophysik, Universität Wien, Türkenschanzstraße 17, A-1180 Wien, Austria*
[8]*Department of Physics and Astronomy, University College London, Gower Street, London WC1E 6BT, UK*
[9]*UK Astronomy Technology Centre, Science and Technology Facilities Council, Royal Observatory, Blackford Hill, Edinburgh EH9 3HJ, UK*
[10]*Institute for Astronomy, University of Edinburgh, Blackford Hill, Edinburgh EH9 3HJ, UK*
[11]*Department of Earth and Space Sciences, Chalmers University of Technology, Onsala Space Observatory, SE-43992 Onsala, Sweden*
[12]*Max-Planck Institut für Radioastronomie, Auf dem Hügel 69, D-53121 Bonn, Germany*
[13]*Department of Physics and Astronomy, University of California, Irvine, CA 92697, USA*
[14]*Leiden Observatory, Leiden University, PO Box 9513, NL-2300 RA Leiden, the Netherlands*

ABSTRACT

We report the first counts of faint submillimetre galaxies (SMGs) in the 870-μm band derived from arcsecond-resolution observations with the Atacama Large Millimeter Array (ALMA). We have used ALMA to map a sample of 122 870-μm-selected submillimetre sources drawn from the $0°.5 \times 0°.5$ the Large Apex BOlometer CAmera (LABOCA) Extended *Chandra* Deep Field South submillimetre survey (LESS). These ALMA maps have an average depth of $\sigma_{870\,\mu m} \sim 0.4$ mJy, some approximately three times deeper than the original LABOCA survey and critically the angular resolution is more than an order of magnitude higher, FWHM of ~ 1.5 arcsec compared to ~ 19 arcsec for the LABOCA discovery map. This combination of sensitivity and resolution allows us to precisely pinpoint the SMGs contributing to the submillimetre sources from the LABOCA map, free from the effects of confusion. We show that our ALMA-derived SMG counts broadly agree with the submillimetre source counts from previous, lower resolution single-dish surveys, demonstrating that the bulk of the submillimetre sources are not caused by blending of unresolved SMGs. The difficulty which well-constrained theoretical models have in reproducing the high surface densities of SMGs, thus remains. However, our observations do show that all of the very brightest sources in the LESS sample, $S_{870\,\mu m} \gtrsim 12$ mJy, comprise emission from multiple, fainter SMGs, each with 870-μm fluxes of $\lesssim 9$ mJy. This implies a natural limit to the star formation rate in SMGs of $\lesssim 10^3$ $M_\odot$ yr^{-1}, which in turn suggests that the space densities of $z > 1$ galaxies with gas masses in excess of $\sim 5 \times 10^{10}$ $M_\odot$ is $< 10^{-5}$ Mpc^{-3}. We also discuss the influence of this blending on the identification and characterization of the SMG counterparts to these bright submillimetre

⋆ E-mail: alexander.karim@durham.ac.uk

sources and suggest that it may be responsible for previous claims that they lie at higher redshifts than fainter SMGs.

Key words: galaxies: abundances – galaxies: evolution – galaxies: formation – galaxies: starburst – galaxies: star formation – submillimetre: galaxies.

1 INTRODUCTION

The first deep surveys for extragalactic submillimetre sources (Smail, Ivison & Blain 1997; Barger et al. 1998; Hughes et al. 1998) uncovered high number densities of submillimetre sources at mJy-flux limits and subsequent spectroscopy determined a median redshift of $z \sim 2.5$ for the radio-detected subset of the submillimetre galaxy (SMG) population (Chapman et al. 2005). At these high redshifts, the submillimetre fluxes of these sources correspond to far-infrared luminosities of $>10^{12-13}$ L$_\odot$, placing them in the ultraluminous or hyperluminous infrared galaxy (ULIRG or HLIRG) classes. These joint 850-μm and radio-selected samples remain the best-studied SMGs and it has been claimed that they host up to half of the star formation occurring at $z \gtrsim 2$ (e.g. Hughes et al. 1998; Blain et al. 1999; Chapman et al. 2005) and may be linked to QSO activity and the formation of massive galaxies at high redshift (e.g. Swinbank et al. 2006; Alexander et al. 2008; Hickox et al. 2012). If true then SMGs are an essential element in models of galaxy formation. In fact, the first theoretical attempts to reproduce basic properties of SMGs, in particular the 850-μm number counts, required radical alteration of the prescription for starbursts in well-constrained galaxy formation models (e.g. Baugh et al. 2005; Granato et al. 2006), demonstrating the potential power of SMGs as a constraint on galaxy evolution theories.

One concern about the use of the 850-μm number counts as a fundamental constraint on galaxy formation models is that these are derived from low spatial resolution (typically $\sim$15–20 arcsec full width at half-maximum, FWHM), single-dish surveys. This low resolution means that it is possible that several faint sources within a beam will appear as a single brighter source, changing the shape of the number counts, most critically by potentially producing a false tail of bright sources. A number of attempts have therefore been made to obtain high angular resolution continuum imaging through interferometric observations of individual submillimetre sources (e.g. Gear et al. 2000; Lutz et al. 2001; Dannerbauer et al. 2002; Younger et al. 2008a,b; Wang et al. 2011) and (nearly) flux-limited samples (Younger et al. 2007, 2009; Barger et al. 2012; Smolčić et al. 2012). These observations have indeed shown that a number of bright submillimetre sources actually comprise emission from multiple SMGs. However, the conclusions from many of these studies have been weakened by a number of factors. First, both the modest numbers of sources studied and the fact that the discovery surveys underlying these studies are typically shallow or restricted to small areas have meant that it has not been possible to conclusively test the shape of the bright-end of the submillimetre source counts. Secondly, many of the follow-up observations of 870 μm-selected submillimetre sources have been carried out at longer wavelengths (typically >1.2 mm). This has led to ambiguous results, especially when comparing the single-dish and interferometer-based fluxes for sources, and so limits the conclusions that can be drawn about their multiplicity. However, one particularly noteworthy study is that recently published by Barger et al. (2012) (see also Wang et al. 2011) which used the Submillimeter Array (SMA) at 850 μm to observe 16 850 μm-selected submillimetre sources with fluxes >3 mJy (>4 σ) from a SCUBA survey of 110 arcmin^2 within the Great Observatories Origins Deep

Survey North (GOODS-N; Giavalisco et al. 2004; Wang, Cowie & Barger 2004). This wavelength-matched study, yielding interferometric resolution of $\gtrsim$2 arcsec, showed the best evidence yet for an increased incidence of multiple SMGs in submillimetre sources at bright 850-μm fluxes. However, better statistics are needed given the small sample and the substantially larger beam of the SMA compared to that of the bolometer might give rise to serendipitous detections not associated with the underlying submillimeter source.

The issue of reliable SMG counts, needed to robustly constrain the theoretical models, is obviously an area where the Atacama Large Millimeter Array (ALMA) will have significant impact. In 2004, we therefore started planning a survey to provide a large, flux-limited sample of submillimetre sources over a wide area in a field with excellent visibility from ALMA. The field chosen was the 0°.5×0°.5 Extended *Chandra* Deep Field South (ECDFS) which has the most extensive multiwavelength coverage of any large-area extragalactic region in the Southern hemisphere. The result was the LABOCA ECDFS submillimetre survey [LESS; Weiß et al. (2009, hereafter W09)], which obtained a deep, $\sigma_{870\,\mu m} \sim 1.2$ mJy, homogeneous 870-μm map of the full ECDFS detecting 126 submillimetre sources.

As the next step, in ALMA Cycle 0 we observed 122 of the 126 submillimetre sources from LESS using ALMA in its compact configuration. These data and the resulting SMG catalogue are presented in Hodge et al. (2013, hereafter H13). Critically, these observations were carried out at the same wavelength as the LABOCA survey. The resulting ALMA maps yield unambiguous identifications for a large fraction of the submillimetre sources, directly pinpointing the SMG(s) responsible for the 870-μm emission to within <0.3 arcsec (e.g. Swinbank et al. 2012). The spatial resolution achieved by our observations ($\sim$1.5 arcsec FWHM) corresponds to an order of magnitude improvement over the single-dish LABOCA survey. It thus provides an ideal data set to determine the influence of multiplicity on the form of the 870-μm SMG counts, as required to enable a reliable comparison to model predictions (e.g. Baugh et al. 2005).

In this paper, we analyse these ALMA maps to derive number counts for SMGs and compare these to both previous source counts from single-dish submillimetre surveys and to predictions from theoretical models. We adopt a cosmology with $\Omega_\Lambda = 0.73$, $\Omega_M = 0.27$ and $H_0 = 72$ km s^{-1} Mpc^{-1} in which a scale of 1 arcsec corresponds to a physical separation of $\sim$8.4 kpc at a redshift of $z = 2$.

2 OBSERVATIONS AND CALIBRATION

Of the 126 submillimetre sources detected in the LESS, 122 were observed during Cycle 0 using the band 7 receivers in ALMA's compact array configuration. The available 8-GHz bandwidth was centred at an observed frequency of 344 GHz (i.e. 870 μm) and we employed a dual polarization setup. This choice of observing frequency enables a direct comparison to the flux densities of the submillimetre sources measured in the original LABOCA survey. The observing campaign was carried out in eight observing blocks (ALMA measurement sets; hereafter MS) between 2011 October
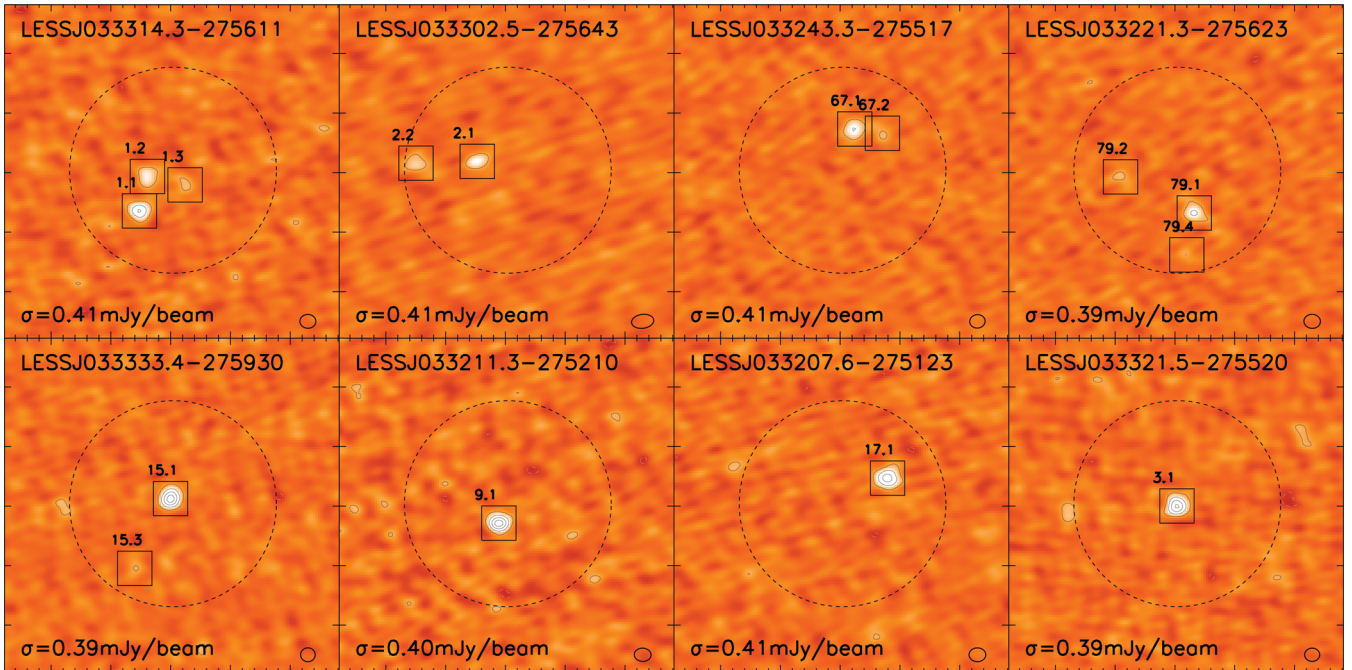
Figure 1. Examples of the 870-μm ALMA continuum maps towards eight of the submillimetre sources from the LESS survey. In each map, we identify all of the sources with S/N > 3.5σ (squares labelled by their catalogue number; see H13). The ALMA data unambiguously locates the SMGs to a precision of <0.3 arcsec and to flux limits of ~2 mJy beam⁻¹ (~3.5–7σ). The upper row shows a selection of maps containing multiple detections, including the maps towards the two brightest LESS sources in our sample (see the text for details). Different SMGs found in a given map are typically separated by >6 arcsec, corresponding to a minimum separation of ≫40 arcsec. The third panel shows the very closest projected distance found in this survey (2.6 arcsec), corresponding to at least ~20 kpc of separation if both sources reside at the same redshift. The lower row shows those maps that contain the individually brightest ALMA SMGs, determining the bright-end of our source counts (see Section 4). Note that these SMGs are not necessarily associated with the brightest LESS sources. Positive (negative) contours on each map are shown in black (white) and start at (−)3σ and are incremented by (−)5σ. The 1σ noise in the map is shown in the bottom-left corner of each panel. Each map is 25.6 arcsec across and we show the primary beam (dotted circle) encompassing the radius at which the ALMA antenna sensitivity drops to 50 per cent, closely resembling the LABOCA beam.

18 and November 3. Typically 15 antennas were available for each block.

The quasar B 0402−362 (J0403−360) was used for phase calibration, and Mars and Uranus have been used to calibrate the absolute flux scale. Bandpass calibration was generally performed using observations of B 0537−441 (J0538−440). Each science field, centred on the catalogued position of a given LESS source from W09, was observed for a total of ~120 s. The data were processed with the Common Astronomy Software Application (CASA; McMullin et al. 2007) and imaged using the CLEAN algorithm within CASA. A detailed description of the raw data and its calibration as well as imaging is presented in H13.

The field of view – defined as the FWHM of the ALMA antenna reception pattern around the phase centre and referred to as primary beam in the following – is 17.3 arcsec in diameter.[1] Each map has a pixel size of 0.2 arcsec and a total extent of 128 pixels in each dimension, sufficient to cover the primary beam and encompass the error-circles of the submillimetre sources from the LESS maps, ≲5 arcsec (W09), even in confused situations. The average root mean square (rms, σ) of the background noise in the maps is σ ~ 0.4 mJy beam⁻¹ – a factor ~3 deeper than the original LABOCA observation. Using natural weighting, we achieve a typical restoring (clean) beam of ~1.8 arcsec × 1.2 arcsec, although a small number of low-elevation (≪30 deg) observations lead to much larger beam ellipticities and the corresponding image products are typically much noisier than our median maps, producing a tail in the noise distribution extending beyond 0.6 mJy beam⁻¹. In the following – unless explicitly stated otherwise – we will focus on the subset of 88 'best' maps selected from two important, but not mutually exclusive, selection criteria: beam-axial ratio < 2 and rms noise level σ < 0.6 mJy beam⁻¹.[2] The distribution of targets between and within each MS was chosen so that problems with the observations of any particular MS would not bias our sample and hence our 'best' sample represents a random sampling of the LESS catalogue, yielding an unbiased view of the properties of submillimetre sources as a function of 870-μm flux. Fig. 1 shows examples of the calibrated and cleaned maps used in this study. The full source catalogue and all maps are presented in H13.

---

[1] Accordingly, the flux density at a given position in the resulting map can be corrected by multiplication with the corresponding factor derived from an inverse 17.3 arcsec FWHM Gaussian. We will note in the following when primary-beam-corrected fluxes are used. Also note that the FWHM used, based on actual beam measurements, is slightly smaller than theoretically expected for a 12-m antenna (in absence of other publicly available information on this matter we refer to ALMA help desk ticket CSV-1014 for further information).

[2] Note that we analyse those maps that do not comply with our selection criteria in the same way as the 88 'best' maps, including the identification of sources as described in the following. Bright sources detected at sufficient significance in those maps form part of a supplementary ALMA catalogue which is not used in this paper unless explicitly stated. See H13 for further details.

3 IDENTIFICATION OF ALMA SOURCES

3.1 Source extraction and characterization

In order to detect SMGs in our calibrated and cleaned maps we use an automated scheme (described in detail in H13). Our IDL-implemented source extraction software first identifies individual signal peaks above a 2.5-σ threshold which are used as the basis to model the emission in that region using a Metropolis–Hastings Markov chain Monte Carlo algorithm to determine the best six-parameter fit for an elliptical Gaussian[3] to describe the underlying flux distribution within a 2 arcsec × 2 arcsec region. This is large enough to recover any extended sources but small enough to resolve double sources. Whilst we attempt a full six parameter fit, at the resolution of our survey (∼1.5 arcsec corresponding to physical scales of ∼12 kpc at $z > 1$), many sources are unlikely to be resolved. We therefore repeat the fitting process using a simple elliptical point-source model with only three free parameters and source extents as well as orientation fixed to the synthesized beam parameters. We find that the peak flux densities from the simple fit generally agree with the integrated flux densities given their full fitting errors, we find a >2σ integrated flux excess in just one source, suggesting it may be resolved. For all other sources, we therefore adopt the peak flux density from the three parameter model as our best estimate of the source flux.

For each parameter in the fit its posterior distribution determines the fitting error, after correcting for autocorrelation in the Markov Chain. These uncertainties are taken into account when determining the full measurement error for the integrated source flux density. The recipes we follow to determine the full uncertainty for elliptical source fits in the presence of correlated noise in radio maps have been motivated by Condon (1997) (see also Windhorst, van Heerde & Katgert 1984; Hopkins et al. 2003; Schinnerer et al. 2004, 2010; Karim et al. 2011).

3.2 Source extraction efficiency and flux recovery

Our goal is to construct a catalogue which is deep, i.e. includes as many real faint sources as possible, but has a very low spurious source fraction. To determine the search parameters necessary to achieve this, we use a suite of simulated ALMA maps. First, we prepare cleaned map which are our actual ALMA maps with all sources >2.5σ identified by our automatic source finder removed. Within the primary beam area of each cleaned map we insert five sources separated from each other by at least two synthesized beam widths. The inserted sources cover a wide range in significance (∼2–20σ) and follow a steeply declining flux density distribution. We then run our code and extract all sources in the simulated maps, in exactly the same fashion as the science maps. We then determine the recovery rate of our inputs sources and how many spurious sources, not associated with any of our model sources,[4] are found. This process is repeated 16 times per map. Thus, in total we insert 7400 sources into the 88 ALMA maps.

Fig. 2 shows the results of our simulations for the fraction of recovered sources and the fraction of detected sources which are
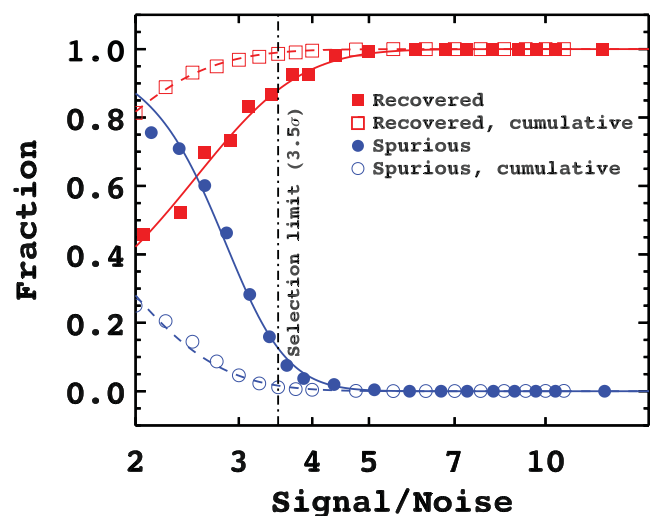

Figure 2. Results from artificial source simulations to test the reliability of our source extraction procedure. After removing >2.5σ sources identified by our automatic source finder, we insert in each map five well-separated sources at random positions within the primary beam, then run our source extraction code and repeat this process 16 times. The red squares denote the fraction of inserted sources that are recovered within a given narrow SNR bin while the blue circles indicate the fraction of extracted sources which are unassociated within 0.8 arcsec with an inserted source. Above the 3.5-σ threshold (vertical dashed black line) – adopted as the reliability limit for our analysis – our catalogue is ∼99 per cent complete and has a false detection rate of ∼1.6 per cent.

spurious, both as a function of measured peak signal-to-noise ratio (SNR). The cumulative distribution shows that the source extraction recovers ∼99 per cent of all >3.5σ sources, while a sample selected above this threshold contains only ∼1.6 per cent spurious detections. We therefore adopt a 3.5-σ detection limit for the sample used in our analysis. With respect to the source extraction efficiency we expect that this sample will contain less than two spurious sources and will fail to include only one intrinsically >3.5-σ source. We also employ the recovered and spurious fractions as a function of detection significance to correct our measured counts in our analysis below. These corrections become significant only below the 3.5-σ catalogue limit and we highlight the flux regime most affected by those corrections when discussing the counts.

As a final test, we compare the total fluxes of the SMGs detected by ALMA to the deboosted fluxes measured for the submillimetre sources in W09. To achieve this, we sum the primary-beam-corrected ALMA fluxes of all sources above a given detection significance, within the ALMA primary beam area, weighted by the LABOCA beam to calculate the total flux that would have been seen by LABOCA at the submillimetre source positions from W09. Since the primary beams of both instruments are very similar, SMGs detected within the ALMA primary beam area contribute to the flux of a given LABOCA source. To our 3.5-σ significance threshold the resulting median ALMA/LABOCA flux density ratio and bootstrap error is $0.83^{+0.09}_{-0.04}$. If the LABOCA flux scale and the flux deboosting of the LESS sources are accurate, this suggests that a contribution from additional fainter SMGs is required to recover the total flux density within the LABOCA beam. Integrating the flux in sources down to a 3-σ significance limit results in a median flux ratio of $0.97^{+0.07}_{-0.04}$, consistent with unity. Given the increasing number of spurious detections at lower detection significance we will, however, retain a 3.5-σ limit for our analysis and discuss the comparison of flux scales in more detail in H13.

---

[3] These six parameters are peak flux density, pixel position of the peak, minor axis extent, axial ratio and position angle.

[4] Below our initial CLEAN threshold our simulated sources are inserted after convolution with the dirty beam instead of the CLEAN beam used for brighter sources. The dirty beam side lobes can then be boosted by noise peaks to appear as spurious sources above our detection limit.

In total, we detect 99 individual SMGs at $>3.5\sigma$ in the 88 maps used. Of these maps, 69 show at least one SMG, 19 maps exhibit two SMGs and four maps have three SMGs within the primary beam. Hence, 19 ALMA maps ($\sim$22 per cent) do not contain a $>3.5\sigma$ source. The associated LABOCA submillimetre sources have a median deboosted flux of 4.5 mJy and a median detection significance of 3.75σ, making these sources amongst the faintest in the LESS survey. The resulting full ALMA SMG catalogue and the exploitation of this catalogue and maps to investigate the multiwavelength properties of the SMGs will be presented in upcoming publications (H13; Simpson et al., in preparation).

4   RESULTS AND DISCUSSION

The ALMA SMGs we have identified can be used to estimate the 870-μm source counts free from the influence of blending. In the following, we describe the derivation of these counts and compare the results to those from previous single-dish surveys.

4.1   Derivation of ALMA 870-μm source counts

We are interested in the differential number counts of SMGs as a function of flux. Our ALMA survey covers submillimetre sources above the flux limit of the LESS discovery survey catalogue (W09) so that the effective ALMA survey area, A_{ALMA}, above this selection limit is given by

$$A_{\text{ALMA}} = \frac{N_{\text{maps}}(\text{ALMA})}{N_{\text{sources}}(\text{W09})} \times A_{\text{LESS}}, \qquad (1)$$

where $N_{\text{maps}}(\text{ALMA}) = 88$ is the number of ALMA maps used in this study, $A_{\text{LESS}} = 0.35$ deg^2 is the LESS survey area and $N_{\text{sources}}(\text{W09}) = 126$ is the total number of submillimetre sources in the LESS catalogue.

Necessarily, this area is only correct in the flux regime covered by the LESS survey.[5] Below the LESS flux limit, the source counts derived from our ALMA maps must be considered biased since the observations were typically taken in the vicinity of a brighter submillimetre source and so are not necessarily representative of the fainter source population. This restriction already applies to the faint-end of our sample of >3.5-σ ALMA SMGs (which are below the LESS catalogue flux limit) and we neither attempt any interpretation of these values nor apply further assumptions. For completeness and purely informational value, we additionally derive differential counts for all >2.5-σ ALMA SMGs.

For the computation of all counts presented here, we take into account the flux uncertainty by randomly assigning fluxes to all sources based on their individual error margins. We thereby assume that the individual error distributions are Gaussian and derive the counts for 1000 resamples. Our best estimate for a given count is given by the mean of all resamples while the standard deviation of which is added in quadrature to the Poissonian error to derive an uncertainty range.

Given our findings in Section 3.2, the source sample and hence the counts are affected by our SNR selection and so we use the recovery and spurious fraction rates derived from our simulations to

correct our observed counts. However, we stress that these extraction biases barely affect our sample and even less so the flux regime above the LESS-detection limit. Our parametrizations (from Fig. 2) of the fractions of spurious detections, $f_{\text{spurious}}(\text{SNR})$, and sources recovered in our simulations, $f_{\text{recovered}}(\text{SNR})$, provide us with the probability that an SMG with a given SNR is spurious and also the likelihood that SMGs of the same SNR are missed. For each SMG, we therefore derive an individual source probability of $p(\text{SNR}) = 2 - f_{\text{recovered}}(\text{SNR}) - f_{\text{spurious}}(\text{SNR})$. Corrected differential source counts for a given resample are then given by the total of all source probabilities in a given flux bin and normalized using equation (1).

Fig. 3 shows the resulting differential as well as the cumulative number counts (summarized in Table 1) along with the corresponding corrected values. The differential source counts derived for our sample ($>3.5\sigma$) are, as expected, only affected by the bias-corrections at the lowest flux densities while the cumulative counts are even less affected. For flux density bins containing <3.5-σ sources – far below the LESS survey limit – we show only bias-corrected values. We also show the best-fitting broken power law to describe our differential counts above the LESS catalogue limit and summarize all these fit parameters in Table 2. The uncertainty range for each parameter is thereby derived by bootstrapping over the parametric fits to all our resamples.

4.2   The absence of the bright SMG population

The most surprising result of our counts is a clear break at the bright-end caused by a lack of bright SMGs in our ALMA maps. None of our maps detect an SMG with a flux $\gtrsim$9 mJy despite 12 sources with 870-μm fluxes $>$9 mJy in the LESS survey. In at least four of these cases, the submillimetre sources comprise multiple (fainter) SMGs. This is particularly clear in the very brightest LESS sources ($\gtrsim$12 mJy; see Fig. 1) where we detect multiple high-significance ($\gg$6σ) SMGs in each map. In the remaining cases, a single ALMA SMG is detected above 3.5σ, although in all cases, the flux density of this SMG significantly underpredicts the LABOCA flux. This shortfall in flux could arise either from our resolving-out extended emission or from the presence of several $\sim$1–1.5-mJy SMGs, which lie below our detection threshold. Nevertheless, an important result of our survey is that the brightest submillimetre sources ($>$9 mJy) in single-dish surveys likely comprise multiple, fainter SMGs.

On average the mutual separations between different SMGs found in a given map are $>$6 arcsec, corresponding to physical scales of $\gg$40 kpc in the typical redshift range and provided that we are dealing with physical and not just projected pairs. The very closest projected distance between two SMGs is 2.6 arcsec as found in only a single map (see Fig. 1), corresponding to at least $\sim$20 kpc of separation if both SMGs reside at the same redshift. Typically, we find that the flux in a map showing multiple detections is distributed in ratios of 70:30 (double detections) and 50:30:20 (triple detections). Given such clear angular separations we indeed need to count each ALMA component as individual SMGs. We note that the scale, orientation and flux ratio of the multiple components are not consistent configurations caused by gravitational lensing and hence unlikely to represent multiply imaged sources.

SMGs with 870-μm fluxes of $>$9 mJy are likely to be HLIRGs (Rowan-Robinson 2000; Rowan-Robinson & Wang 2010) if they lie at $z > 1$. The lack of large numbers of such bright SMGs in our sample then implies a natural limit to the star formation rate (SFR) in an SMG of $\lesssim$10^3 M$_\odot$ yr^{-1} [for a Salpeter (1955) IMF]. This maximal SFR is driven by the ratio of the mass of the available gas reservoir and the free-fall time of the system (Lehnert &

---

[5] Strictly speaking, this area is only valid for sources in the phase centre of a given ALMA map since the sensitivity monotonically drops to 50 per cent at the primary-beam radius. Nevertheless, for the interesting regime of our analysis – above the LESS survey flux limit – even at half the phase centre sensitivity sources would be detected at a >3.5-σ level and hence included in our analysis even if residing right at the edge of our field of view.
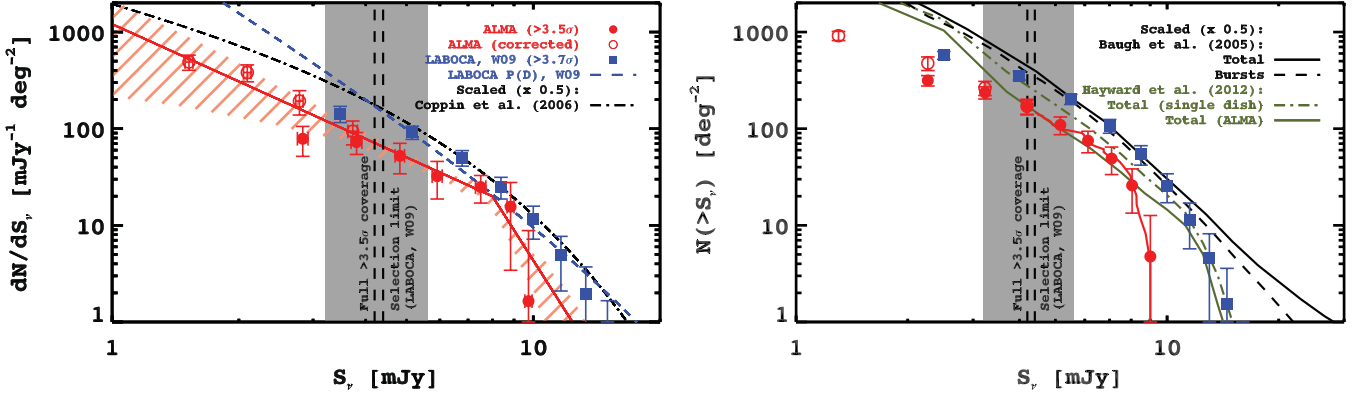
Figure 3. Left: the primary-beam-corrected differential 870-µm source counts from our ALMA survey. Above the LESS survey limit (depicted with a shaded margin representing the LABOCA rms), the counts of ALMA SMGs should be a true representation of the actual population and any SMG that contributed to the LABOCA source will have been included in our analysis. We also plot counts below this limit for our robust ALMA sample (all bins depicted by the filled circles comprise >3.5-σ detections) which is largely uncontaminated by spurious sources while showing a high detection efficiency (see Fig. 2). In addition, we extend the counts to >2.5-σ significance applying the larger corrections necessary for the fractions of spurious and undetected sources. Fainter than ∼9 mJy our data are slightly lower but in reasonable agreement – within the error margins – with the scaled fit (scaling adopted from W09) to the number counts from the SHADES survey (Coppin et al. 2006). However brighter than ∼9 mJy, we find a steeper decline than shown in the single-dish counts (a Schechter (1976) parametrization of the differential counts resulting from an P(D) analysis of the LESS map by W09 similarly overpredicts the bright counts). Submillimetre sources brighter than this limit were detected by the LESS survey (deboosted values) but no comparably bright SMG is observed by ALMA. Instead, the ALMA maps of the brightest LESS sources show an increase in source multiplicity. To parametrize our counts, we fit a broken power law to the data above the LESS survey limit (see Table 2), shown by a red solid line and light red shaded error margins. Right: corresponding cumulative counts of >3.5-σ ALMA sources compared to the deboosted LESS results and the Baugh et al. (2005) model predictions. The latter are constrained by observed data from single-dish submillimetre surveys and the predicted fraction of bursts is shown in addition to the total counts. Scaled to the LESS data, the model is comparable to our results above the selection limit while the clear mismatch at the bright-end due to the absence of corresponding ALMA SMGs is apparent. The scaled Hayward et al. (2013) model, designed to predict the ALMA counts, accounts reasonably for source blending effects but also fails to reproduce the bright-end. The cumulative counts are corrected for the fraction of missing/spurious detections, but this has a minor effect on our sample due to its high cumulative detection efficiency.

Table 1. Differential and cumulative counts of 870-µm ALMA-detected SMGs.

⟨S_ν⟩ (mJy)	Differential dN/dS_ν (mJy^{-1}deg^{-2})	S_ν (mJy)	Cumulative N(> S_ν) (deg^{-2})
4.8 (0.1)	52.3 (18.2)	4.2	167.3 (28.6)
5.9 (0.2)	32.3 (13.6)	5.2	109.4 (22.8)
7.5 (0.2)	24.9 (7.9)	6.1	75.2 (18.8)
8.8 (0.2)	15.6 (12.2)	7.1	49.1 (15.5)
9.7 (0.2)	1.6 (7.2)	8.0	25.9 (12.5)
11.0	0.0	9.0	4.8 (7.9)
14.0	0.0		

Notes: Differential (left) and cumulative (right) 870-µm SMG counts down to the LESS survey catalogue selection limit as shown in Fig. 3. The counts throughout the entire flux regime do not require any correcting assumptions. The 1-σ uncertainty ranges stated in parentheses are based on the corresponding standard deviations obtained in 1000 Monte Carlo realizations of our catalogue according to the flux uncertainties of individual sources (see Section 4.1 for details). The Poissonian uncertainty is additionally taken into account.

Table 2. Parametrized fit to the differential counts of 870-µm ALMA-detected SMGs.

dN/dS_ν [1/N^*]	N^* (mJy^{-1} deg^{-2})	S_ν^* (mJy)	α	β
$\left(\frac{S_\nu}{S_\nu^*}\right)^{-\alpha}$, $S_\nu < S_\nu^*$				
$\left(\frac{S_\nu}{S_\nu^*}\right)^{-\beta}$, $S_\nu \geq S_\nu^*$	20^{+14}_{-15}	8	$2.0^{+0.5}_{-0.4}$	$6.9^{+2.8}_{-2.3}$

Notes. Best-fitting broken-power-law parameters to describe our data. The fit is applied only to the data above the LESS catalogue limit and provides a good representation of the steepness of the bright-end of our SMG counts (above the fixed breaking point of 8 mJy). We urge caution when extrapolating this parametrization to much fainter fluxes.

of <10^{-5} Mpc^{-3}. For normal star-forming $z < 3$ galaxies, Karim et al. (2011) suggest that their inverse free-fall time constitutes a potential upper limit to their specific SFR. Assuming a typical stellar mass of ∼10^{11} M$_\odot$ for our SMGs (e.g. Swinbank et al. 2012), we also find that their specific SFR is in agreement with this upper limit.

We therefore parametrize the differential counts with a double power law with a break point. Since our data coverage of the regime brighter than the LESS survey limit is really too sparse for a four-parameter model fit, we choose to fix the break point at 8 mJy. Fitting this model, we find a factor of >3 difference in the power-law indices of the two power-law components (see Table 2). A simple step function would also provide a reasonable representation of our data while not significantly changing the result.

Although previous interferometric surveys of submillimetre sources cannot be considered complete as they comprise a

Heckman 1996). For a free-fall time of ∼50 Myr as found by Kennicutt (1998) for local starbursts, the implied cold gas mass limit is ≲5 × 10^{10} M$_\odot$. This is comparable to the limiting gas mass for SMGs found by Bothwell et al. (2013). Integrating the parametrization of our differential counts under consideration of the error margins, the absence of very bright SMGs in the LESS survey area therefore suggests that high-redshift galaxies with cold gas masses significantly above 5 × 10^{10} M$_\odot$ have space densities

complex mix of follow-up observations from heterogeneous surveys and small survey fields, it is instructive to compare our findings to these previous results. For example, Barger et al. (2012) obtained deep integrations of four $\gtrsim$10 mJy SMGs in GOODS-N with the SMA at 860 μm and showed that at least one breaks up into multiple components across ∼5 arcsec. Earlier results by Wang et al. (2011) also suggested that potentially ∼30 per cent of >5-mJy 850-μm sources could comprise such multiple systems, potentially rising to >90 per cent above ∼8 mJy (see also Wang et al. 2007; Younger et al. 2008a; Cowie et al. 2009; Smolčić et al. 2012).

These results support our interpretation that the number of bright submillimetre sources $\gtrsim$9 mJy from single-dish surveys have been substantially overestimated, producing artificially high SMG number counts at the brightest fluxes. To highlight this, we show in Fig. 3 the results from W09 and those from the SCUBA HAlf Degree Extragalactic Survey (SHADES; Coppin et al. 2006) scaled to the LESS data as described by W09. We refer to both studies for an extensive comparison to other ∼850-μm single-dish surveys. It is noteworthy that even sophisticated methods to estimate the differential source counts from single-dish submillimetre surveys – such as the probabilistic $P(D)$ analysis presented by W09 – still recover a false excess of bright sources (see Fig. 3). In order to derive the true counts, this $P(D)$ analysis, which derives the differential counts solely from the flux distribution in the map and not based on individually extracted sources, would need to account for the clustering of sources on small angular scales. A similar bias may also be present at intermediate flux levels, where our counts are not significantly lower than the single-dish results, as would be necessary if source numbers were conserved above our flux limit. This may be hinting that these fainter sources also suffer from multiplicity effects. Moreover, some of the ALMA maps of fainter LABOCA sources which lack >3.5-σ SMGs may then be explained by the presence of multiple SMGs below our detection limit.[6] Hence, the statistical prediction by W09 of only five LESS sources being spurious may still be valid.

The high multiplicity of the brightest submillimetre sources also has wider implications. For example, it has been claimed that the brightest (most luminous) SMGs evolve more strongly than fainter systems and hence are preferentially found at the highest redshifts (e.g. Ivison et al. 2002, 2007; Wall, Pope & Scott 2008; Marsden et al. 2011; Smolčić et al. 2012). This could now simply be explained by two effects: confusion, which nullifies the statistical techniques used to identify counterparts, meaning that the very brightest submillimetre sources lack obvious counterparts at other wavelengths and as a result are associated with (undetectable) high-redshift sources; and the significant overestimation of the submillimetre fluxes for the identified counterparts, whose artificially enhanced radio/submillimetre flux ratios then mimic those expected for high-redshift SMGs.

Similarly, the detection rate of ^{12}CO emission in the SMG survey of Bothwell et al. (2013) declines with 850-μm flux. For example, from their sample of 40 SMGs, the eight of which are undetected (including 2/5 with $S_{850} \geq$ 10 mJy) in ^{12}CO have a median $S_{850} =$ 8.1 ± 0.7 mJy, compared to $S_{850} =$ 5.9 ± 0.7 mJy for the ^{12}CO detections (this is significant at 92 per cent confidence level). This modest difference would be explained if a higher fraction of the brighter sources have their submillimetre fluxes boosted by emission

from other sources projected along the line of sight within the beam. This scenario is consistent with the suggestion of Wang et al. (2011) that where several SMGs comprise a submillimetre source, those individual components are not necessarily physically associated.

The high multiplicity of bright submillimetre sources may also bias the form of the far-infrared–radio correlation, which is widely used to infer SFR out to high redshifts. For example, where the submillimetre flux of a source is derived from single-dish photometry, and in fact represents contributions from several SMGs, with the radio emission coming from a single source, then this will produce a systematic offset and scatter in the derived far-infrared–radio correlation. A number of studies (e.g. Ibar et al. 2008; Ivison et al. 2010; Sargent et al. 2010; Bourne et al. 2011) have attempted to trace the evolution of this relation over a range of redshifts, of which several focused on submillimetre-bright sources (e.g. Kovács et al. 2006; Murphy et al. 2009; Murphy 2009). The latter reported a radio excess for submillimetre-selected sources compared to local star-forming galaxies and – if true – this offset would increase further if only a single subcomponent is associated with the radio emitter.[7] However, we postpone a discussion of the radio properties of our ALMA SMGs to an upcoming publication.

Finally, we also compare our SMG counts in Fig. 3 to the predicted counts from the model of Baugh et al. (2005) which, by design, match the single-dish observations. In comparison, consequently, our counts are significantly lower, particularly at the bright-end. Since Baugh et al. (2005) could only reproduce the submillimetre counts by including a top-heavy initial mass function (IMF) during bursts of star formation, the tension created by our ALMA counts might aid the model to reproduce the true counts without resorting to a non-standard IMF. However, our data show no strong disagreement at intermediate fluxes so that the fundamental problem for models of reproducing the normalization of the counts may still persist.[8] Recently, Hayward et al. (2013) predicted the submillimetre source counts by a combined semi-analytical/hydrodynamic approach without including a top-heavy IMF for bursts. Throughout the flux regime covered by our study, they predict a consistently high fraction (>30 per cent) of galaxy pairs, in agreement with our observations. Still, their predicted bright SMG counts do not drop as sharply as our data indicate, since our fraction of multiple sources steeply rises at the bright-end.[9] At fluxes below the break and the above the LESS survey limit, Fig. 3 shows that their model reproduces the marginal difference between the counts at interferometric and single dish resolution as a result of blended, physically separated not interacting galaxy pairs, in agreement with our study. It should be noted, however, that in contrast to, e.g., the Baugh et al. (2005) model the predictive power of the Hayward et al. (2013) work is limited to the submillimetre properties of distant star-forming galaxies, as it is not required to reproduce the global population of galaxies, particularly in the local Universe.

---

[6] Assuming standard dust properties a galaxy at $z > 1$ with an SFR of 100 M$_\odot$ yr^{-1} would have an 870-μm flux of ∼1 mJy, below our detection limit. For a detailed discussion we refer the reader to H13.

[7] It should be noted that Barger et al. (2012) find that five of their SMA sources agree with the local relation.

[8] For example, Fontanot et al. (2007) highlight the difficulty of semi-analytical models to simultaneously reproduce the abundance of SMGs and $z \lesssim 1$ massive galaxies when a standard IMF is used.

[9] For a detailed analysis of the source multiplicity as a function of flux we refer the reader to H13. Note that the interferometric follow-up of LABOCA sources in the Cosmic Evolution Survey (COSMOS) field presented by Smolčić et al. (2012) shows a similarly elevated fraction of multiple sources at the bright-end.

5 SUMMARY

We have presented source number counts derived from an 870-µm ALMA survey of submillimetre sources from the 870-µm LABOCA survey of the ECDFS by W09. Compared to the parent survey, our ALMA maps are three times deeper and have an angular resolution which is an order of magnitude higher, allowing us to remove the influence of blending on the counts above the LABOCA detection limit. We find that our source counts are in broad agreement with those of the LABOCA survey and the previous literature results. However, brighter than ~8 mJy, our counts show a deficit of sources compared to those from single-dish surveys. This is caused by multiple SMGs, which are found to be well separated (typically by ~6 arcsec) at the ~1.5 arcsec resolution of our ALMA maps, being blended into single sources at the resolution of the single-dish surveys. This trend has also been seen in recent studies of smaller samples of submillimetre sources. Our results suggest that multiplicity in submillimetre sources is significant at the brightest fluxes, but may also influence fainter submillimetre sources, ~4 mJy, from single-dish surveys. The absence of bright SMGs in our sample implies a limit to the maximum SFR in an SMG of $\lesssim 10^3$ M$_\odot$ yr^{-1} (for a Salpeter IMF), which in turn suggests that systems with gas masses in excess of ~5 × 10^{10} M$_\odot$ have space densities of <10^{-5} Mpc^{-3} at $z \gtrsim 1$.

REFERENCES

Alexander D. M. et al., 2008, ApJ, 687, 835
Barger A. J., Cowie L. L., Sanders D. B., Fulton E., Taniguchi Y., Sato Y., Kawara K., Okuda H., 1998, Nat, 394, 248
Barger A. J., Wang W.-H., Cowie L. L., Owen F. N., Chen C.-C., Williams J. P., 2012, ApJ, 761, 89
Baugh C. M., Lacey C. G., Frenk C. S., Granato G. L., Silva L., Bressan A., Benson A. J., Cole S., 2005, MNRAS, 356, 1191

Blain A. W., Kneib J.-P., Ivison R. J., Smail I., 1999, ApJ, 512, L87
Bothwell M. S. et al., 2013, MNRAS, 429, 3047
Bourne N., Dunne L., Ivison R. J., Maddox S. J., Dickinson M., Frayer D. T., 2011, MNRAS, 410, 1155
Chapman S. C., Blain A. W., Smail I., Ivison R. J., 2005, ApJ, 622, 772
Condon J. J., 1997, PASP, 109, 166
Coppin K. et al., 2006, MNRAS, 372, 1621
Cowie L. L., Barger A. J., Wang W.-H., Williams J. P., 2009, ApJ, 697, L122
Dannerbauer H., Lehnert M. D., Lutz D., Tacconi L., Bertoldi F., Carilli C., Genzel R., Menten K., 2002, ApJ, 573, 473
Fontanot F., Monaco P., Silva L., Grazian A., 2007, MNRAS, 382, 903
Gear W. K., Lilly S. J., Stevens J. A., Clements D. L., Webb T. M., Eales S. A., Dunne L., 2000, MNRAS, 316, L51
Giavalisco M. et al., 2004, ApJ, 600, L93
Granato G. L., Silva L., Lapi A., Shankar F., De Zotti G., Danese L., 2006, MNRAS, 368, L72
Hayward C. C., Narayanan D., Kereš D., Jonsson P., Hopkins P. F., Cox T. J., Hernquist L., 2013, MNRAS, 428, 2529
Hickox R. C. et al., 2012, MNRAS, 421, 284
Hodge J. et al., 2013, ApJ, submitted (H13)
Hopkins A. M., Afonso J., Chan B., Cram L. E., Georgakakis A., Mobasher B., 2003, AJ, 125, 465
Hughes D. H. et al., 1998, Nat, 394, 241
Ibar E. et al., 2008, MNRAS, 386, 953
Ivison R. J. et al., 2002, MNRAS, 337, 1
Ivison R. J. et al., 2007, MNRAS, 380, 199
Ivison R. J. et al., 2010, A&A, 518, L35
Karim A. et al., 2011, ApJ, 730, 61
Kennicutt R. C., Jr, 1998, ApJ, 498, 541
Kovács A., Chapman S. C., Dowell C. D., Blain A. W., Ivison R. J., Smail I., Phillips T. G., 2006, ApJ, 650, 592
Lehnert M. D., Heckman T. M., 1996, ApJ, 462, 651
Lutz D. et al., 2001, A&A, 378, 70
Marsden G. et al., 2011, MNRAS, 417, 1192
McMullin J. P., Waters B., Schiebel D., Young W., Golap K., 2007, in Shaw R. A., Hill F., Bell D. J., eds, ASP Conf. Ser. Vol. 376, Astronomical Data Analysis Software and Systems XVI. Astron. Soc. Pac., San Francisco, p. 127
Murphy E. J., 2009, ApJ, 706, 482
Murphy E. J., Chary R.-R., Alexander D. M., Dickinson M., Magnelli B., Morrison G., Pope A., Teplitz H. I., 2009, ApJ, 698, 1380
Rowan-Robinson M., 2000, MNRAS, 316, 885
Rowan-Robinson M., Wang L., 2010, MNRAS, 406, 720
Salpeter E. E., 1955, ApJ, 121, 161
Sargent M. T. et al., 2010, ApJS, 186, 341
Schechter P., 1976, ApJ, 203, 297
Schinnerer E. et al., 2004, AJ, 128, 1974
Schinnerer E. et al., 2010, ApJS, 188, 384
Smail I., Ivison R. J., Blain A. W., 1997, ApJ, 490, L5
Smolčić V. et al., 2012, A&A, 548, A4
Swinbank A. M., Chapman S. C., Smail I., Lindner C., Borys C., Blain A. W., Ivison R. J., Lewis G. F., 2006, MNRAS, 371, 465
Swinbank A. M. et al., 2012, MNRAS, 427, 1066
Wall J. V., Pope A., Scott D., 2008, MNRAS, 383, 435
Wang W.-H., Cowie L. L., Barger A. J., 2004, ApJ, 613, 655
Wang W.-H., Cowie L. L., van Saders J., Barger A. J., Williams J. P., 2007, ApJ, 670, L89
Wang W.-H., Cowie L. L., Barger A. J., Williams J. P., 2011, ApJ, 726, L18
Weiß A. et al., 2009, ApJ, 707, 1201 (W09)
Windhorst R. A., van Heerde G. M., Katgert P., 1984, A&A, 58, 1
Younger J. D. et al., 2007, ApJ, 671, 1531
Younger J. D. et al., 2008a, MNRAS, 387, 707
Younger J. D. et al., 2008b, ApJ, 688, 59
Younger J. D. et al., 2009, ApJ, 704, 803

This paper has been typeset from a TeX/LaTeX file prepared by the author.